DOI: 10.1002/cphc.201100055

Defect-Assisted Covalent Binding of Graphene to an Amorphous Silica Surface: A Theoretical Prediction

Kyoung E. Kweon[b] and Gyeong S. Hwang*[a]

We propose a mechanism for defect-assisted covalent binding of graphene to the surface of amorphous silica (a-SiO_2) based on first-principles density functional calculations. Our calculations show that a dioxasilirane group (DOSG) on a-SiO_2 may react with graphene to form two Si–O–C linkages with a moderate activation barrier ($\approx$0.3 eV) and considerable exothermicity ($\approx$1.0 eV). We also examine DOSG formation via the adduction of molecular O_2 to a silylene center, which is an important surface defect in a-SiO_2, and briefly discuss modifications in the electronic structure of graphene upon the DOSG-assisted chemical binding onto the a-SiO_2 surface.

1. Introduction

Graphene, a two-dimensional hexagonal allotrope of carbon, exhibits unique physical and chemical properties.[1] Its discovery has opened up interesting possibilities for various future technical applications. While the production of large-area high-quality graphene sheets is technically very challenging, the recently developed transfer printing methods allow for precise patterning of graphene.[2,3] In this approach, a stamp is used to cut and exfoliate graphene sheets from highly oriented pyrolytic graphite and these sheets are then placed onto a substrate of interest. Amorphous silica (a-SiO_2) is an important support for graphene in various applications.[1,4] However, the a-SiO_2 surface frequently needs to be modified to assist graphene detachment from the stamp and binding onto the a-SiO_2 support. Earlier experiments demonstrated that oxygen plasma treatment or chemical functionalization can enhance the interaction of graphene with a-SiO_2.[2] Graphene sheets are also deposited on the defect-free SiO_2 surface,[3] but the weakly physisorbed graphene can easily be removed by solvent washing or sonification.[5] Besides immobilizing it, the graphene–SiO_2 binding interaction may alter the properties of graphene.

Despite its importance, the interaction between graphene and a-SiO_2 is not yet clearly understood, particularly in the presence of defects and chemical functional groups on a-SiO_2. While direct characterization of the interfacial interaction currently appears to be rather limited, computational approaches can serve as a powerful tool. Even so, there have been only a few theoretical studies that focus mainly on crystalline SiO_2 (c-SiO_2).[6–8] Considering that a-SiO_2 might show distinctly different surface properties from c-SiO_2 in association with surface defects and strained Si–O bonds, it is necessary to examine the nature of the a-SiO_2 surface and the effects of surface modifications on the interaction with graphene.

Herein, we present the reaction between graphene and a-SiO_2 that contains a dioxasilirane group (DOSG) on the surface, based on density functional theory (DFT) calculations. The existence of DOSG has also been evidenced by experiments.[9] Earlier studies[10–13] suggested that DOSG can be created by the adduction of molecular O_2 onto the terminal Si of a silylene center, while the silylene center is well known to be an important surface defect in a-SiO_2.[14,15] Minimum energy paths and energetics for the O_2 adduct and graphene binding reactions are determined using a combination of cluster and periodic slab DFT calculations. Modifications in the electronic structure of the DOSG-bound graphene as compared to a free-standing graphene are also examined by calculating electronic density of states.

Computational Methods

The calculations reported herein were performed on the basis of DFT within the generalized gradient approximation (GGA-PW91[16]), as implemented in the Vienna ab initio Simulation Package (VASP).[17] For some selected cases, GGA-PBE[18] and LDA[19] calculations were also performed to look at the effect of exchange–correlation functionals. The projector augmented wave (PAW) method with a plane-wave basis set was used to describe the interaction between ion cores and valence electrons.[20] We used a 60-atom rectangular graphene sheet with dimensions of 12.8163 $\times$ 12.3325 Å^2 in slab calculations and a 72-atom hexagonal graphene sheet in cluster calculations; here, the GGA-optimized lattice constant of 2.467 Å was employed, which is slightly larger than the experimental value of 2.461 Å. The silylene defect on the a-SiO_2 surface was modeled using both slab and cluster models. For the slab-model approach, we constructed three a-SiO_2 slabs with a thickness of about 10 Å using combined Metropolis Monte Carlo and DFT calculations. Each slab consisted of 36 SiO_2 units with a silylene center (corresponding to a missing O atom) on the top sur-

[a] Prof. G. S. Hwang
Department of Chemical Engineering
University of Texas at Austin, Austin, Texas 78712 (USA)
Fax: (+1) 512-471-7060
E-mail: gshwang@che.utexas.edu

[b] K. E. Kweon
Department of Electrical and Computer Engineering
University of Texas at Austin, Austin, Texas 78712 (USA)

 © 2011 Wiley-VCH Verlag GmbH & Co. KGaA, Weinheim

face. The slab's lateral (x and y) dimensions were adjusted to match corresponding graphene dimensions. Further details regarding the construction of a-SiO_2 slabs can be found in refs. [14] and [21]. Periodic boundary conditions were employed in all three directions with a vacuum gap of 8–10 Å in the vertical (z) direction to separate the graphene/a-SiO_2 system from its periodic images. During geometry optimization (energy minimization), all atoms were fully relaxed using a conjugate gradient method until residual forces on constituent atoms become smaller than 4×10^{-2} eV Å^{-1}. In geometry optimization, we employed a plane-wave cutoff energy of 408 eV and a (3×3×1) k-point grid in the scheme of Monkhorst–Pack for the Brillouin zone sampling,[22] and an increased k-point mesh size up to (12×12×1) to refine the calculations of corresponding electron density of states (DOS) and partial charge densities. A higher cutoff energy of 450 eV and a k-point mesh of (7×7×1) were used for grid-based Bader charge analysis.[23] The convergence of the atomic and electronic structure calculations was also carefully checked with respect to supercell size. Reaction pathways and barriers were determined using the climbing-image nudged elastic band method (c-NEBM)[24] with 6–8 intermediate images for each elementary step.

2. Results and Discussion

The scheme in Table 1 shows a defect-assisted mechanism that we propose for the covalent binding of graphene to the surface of a-SiO_2. If a silylene center [a; $(\equiv Si{-}O)_2Si$, where $-$ represents a Si–O bond] exists on a-SiO_2, O_2 may easily adsorb on the active silylene site (SS) and form a dioxasilirane group (DOSG) [b; $(\equiv Si{-}O)_2Si<O_2$]. Then, the DOSG may react with two adjacent C atoms in the graphene sheet and form a five-membered ring [c; $(\equiv Si{-}O)_2Si<(O{-}C)_2$ indicated as DOSG/Gr hereafter]. Herein, three independent a-SiO_2 slabs (each of which has a SS on the surface) were constructed to consider the strain effects associated with the disordered structure of a-SiO_2. For comparison, we also performed cluster calculations that can minimize the strain contribution. Table 1 summarizes the geometric parameters and reaction energies predicted by our GGA-PW91 calculations. Our slab (cluster) calculations predict the overall reaction to be exothermic by 3.96–4.13 (4.34) eV, suggesting that graphene can be strongly bound to the chemically modified a-SiO_2 surface by forming Si–O–C linkages. Here we should point out that the DFT slab calculations underestimate the dispersion interaction between the graphene and SiO_2 substrate, and moreover, the cluster approach neglects the graphene–SiO_2 interaction. According to the GGA-PW91, the graphene–SiO_2 interaction energy is predicted to be of the order of 1 meV Å^{-2} at the distance of 3.4 Å, which is smaller than about 6 meV Å^{-2} as estimated for the corresponding van der Waals interaction.[4] As such, ΔE_2 values (in Table 1) are somewhat underestimated as a result of the tendency of the DFT-GGA calculation to underestimate long-range dispersion interactions. Next, we discuss each reaction step in detail.

Figure 1 (left panels) shows the minimum-energy configurations of SS, DOSG, and DOSG/Gr determined using SLAB B (see Table 1), together with the corresponding optimized model clusters (right panels). For the SS (a), the Si–O bond distance and the O–Si–O bond angle slightly vary from 1.68–1.69 Å and 107–112° in the slab calculations to 1.65 Å and 103° in the cluster calculation. The divalent Si in the singlet state has one lone pair which is aligned along the bisector of the O–Si(:)–O angle. Due to the repulsion between the lone electron pairs on Si and O, the Si–O bond tends to be slightly elongated compared to the calculated mean Si–O bond length of 1.63 Å in bulk a-SiO_2. Given that Si prefers sp^3 hybridization rather than sp^2 hybridization, we can expect that the planar silylene center is highly reactive.[13]

An O_2 molecule may readily react with the active divalent Si in SS and form a DOSG (Figure 1 b), that is, O_2 (triplet) + SS (singlet)→DOSG (singlet). Previous studies[12,26–28] suggest that the O_2 adduct reaction would follow three steps. Firstly, one end of the O_2 binds to the divalent Si and forms a silanone O-oxide (>Si•OO•, where • represents a dangling bond) in which the Si becomes pyramidalized (like a silyl radical, ≡Si•) while the Si-bound O_2 (Si–OO•) exhibits superoxo (O_2^-) character. The silanone O-oxide is likely to have triplet diradical character. Secondly, the silanone O-oxide (>Si•OO•) undergoes spin conversion to a lower-lying singlet state. Thirdly, subsequent cyclization (or ring closure) leads to the formation of DOSG with a three-membered ring. From our slab (cluster) calculations the overall exothermicity of the O_2 adduction is predicted to be 3.1–3.2 (3.3) eV, consistent with previous theoretical studies that also reported high exothermicities of 2.7–4.1 eV, depending on the silylene substituents (such as :SiX_2, X = H, CH_3, Ph).[11,26,27] In addition, the O_2 adduct reaction tends to occur with no significant activation barrier. For instance, the reaction between SiH_2 and O_2 was observed to occur at 297–600 K.[12]

For the singlet DOSG (b), the predicted O–O/Si–O bond distances and O–Si–O bond angle are 1.64 (1.63)/1.64 (1.65) and

Table 1. Optimized geometrical parameters for a) silylene site (SS), b) dioxasilirane group (DOSG), and c) DOSG/graphene (DOSG/Gr) and calculated total energy changes for the SS + O_2 (ΔE_1) and DOSG + Gr (ΔE_2) reactions from cluster and periodic slab DFT-GGA (PW91) calculations. In the slab calculations, three independent slab models were employed. The distances (d) and angles (θ) are given in Å and degree [°], respectively. The energy values (ΔE_1, ΔE_2) are in eV; the negative sign indicates energy gain during the reaction.

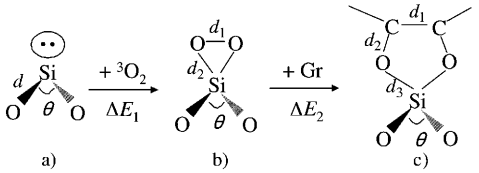

a) b) c)

	d	θ	d_1/d_2	θ	$d_1/d_2/d_3$	θ	ΔE_1	ΔE_2
SLAB A	1.69	112.3	1.64/1.64	116.3	1.59/1.50/1.64	114.6	−3.16	−0.80
SLAB B	1.69	111.5	1.64/1.64	116.5	1.60/1.50/1.63	115.6	−3.20	−0.93
SLAB C	1.68	106.7	1.64/1.64	112.5	1.58/1.50/1.63	111.5	−3.14	−0.85
Cluster	1.65	102.6	1.63/1.65	107.9	1.60/1.49/1.65	108.2	−3.30	−1.04

 © 2011 Wiley-VCH Verlag GmbH & Co. KGaA, Weinheim

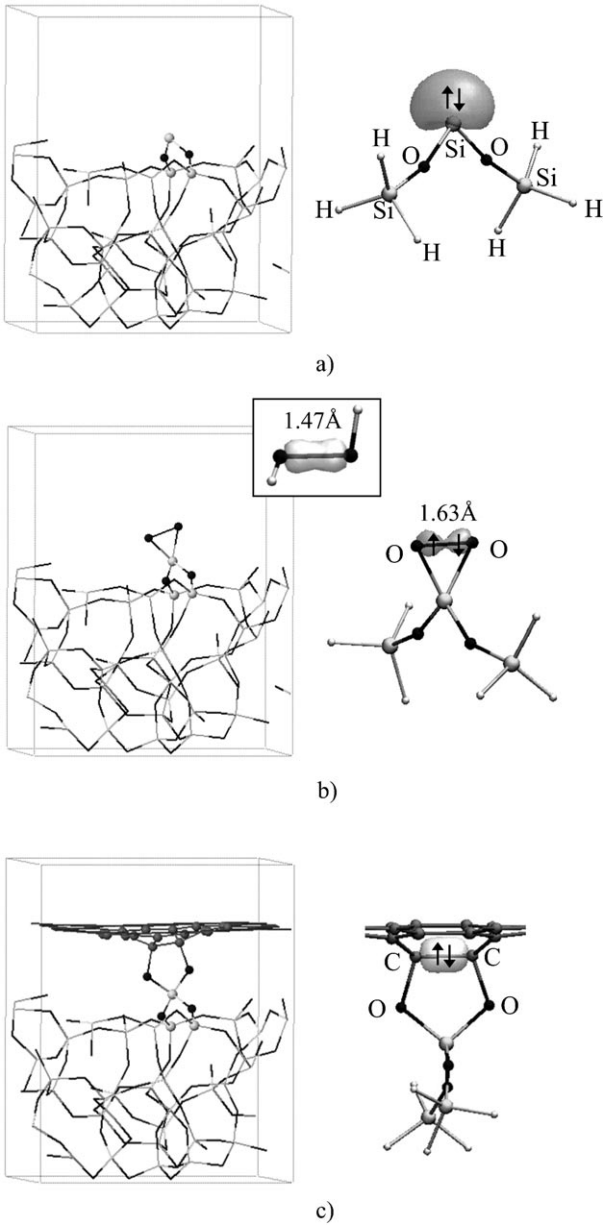

Figure 1. Optimized configurations of a) silylene site (SS), b) dioxasilirane group (DOSG), and c) DOSG/graphene (DOSG/Gr) determined using SLAB B (left panels) and model clusters (right panels). The inset in (b) shows a HOOH molecule for comparison. Wireframe represents bulk Si and O atoms in the *a*-SiO_2 lattice. The lone electron pair in SS (a), the O–O bonds in DOSG and HOOH (b), and the C–C bond in DOSG/Gr (c) are represented by the maximally localized Wannier functions, which were calculated using the CPMD package.[25] The isosurface values in (a), (b), and (c) are 0.70, 1.94, and 1.40 electron $Å^{-3}$, respectively. The light gray, dark gray, (small) white, and gray balls represent Si, O, H, and C, respectively, as also indicated.

113–117° (108°), respectively, from our slab (cluster) calculations, in good agreement with previous calculations.[11,29] The elongated O–O bond, compared to 1.47 Å for peroxo (in HOOH), can be ascribed to the highly strained three-membered ring.[12,28] The resulting weakening of the O–O bond is also well demonstrated by the distinctive dumbbell-shaped isosurface of the corresponding Wannier function (Figure 1 b), as compared to the case of HOOH (inset in Figure 1 b). We also estimated atomic charges in DOSG using Bader charge analysis with special care for convergence with respect to charge density grid. The result clearly demonstrates charge transfer to the attached O_2 (approximately 0.8e per O atom), suggesting that DOSG might have the character of singlet biradicals.[28]

Next, we examined the reaction of DOSG with graphene. As shown in Figure 1 c, a DOSG can be chemically bound to graphene by forming two C–O–Si linkages, resulting in a pentagonal ring analogous to the ethylene reaction with DOSG.[12] This reaction involves rupture of a π bond in graphene and formation of two C–O bonds. The sp^3-like C atoms are pulled down by $\approx$0.9 Å and the C–C–O and C–O–Si bond angles are 107° and 113°, respectively (from our cluster calculations). As listed in Table 1, the C–C bond length of 1.60 Å is slightly greater than the calculated value of 1.55 Å for a C–C single bond in the tetrahedral diamond lattice.

Figure 2 shows a viable route that we have identified for the DOSG + Gr → DOSG/Gr reaction using the cluster approach, together with an energy variation along the reaction coordinate. Here, the $O_2 > Si(OSiH_3)_2$ cluster (as shown in Figure 1 b) was used to mimic the DOSG. Given the singlet initial (A) and final (E) states, the reaction is assumed to occur on the singlet potential energy surface according to the spin conservation rule.[27] Initially, the graphene was placed 3.3 Å above the O–O dimer of DOSG, close to a typical van der Waals distance. In the initial state A, the DOSG–Gr interaction energy is predicted to be 0.05 eV with respect to the fully separated DOSG cluster and graphene sheet (FS), while the O–O bond is slightly elongated compared to the isolated DOSG case.

As presented in Figure 3, the electronic density of states (DOS) analysis shows that the lowest unoccupied energy state of DOSG (inset) is located slightly above the valence band edge of pristine graphene (a), allowing charge transfer from the graphene sheet to the DOSG. The DOS were calculated using the tetrahedron method with Blöchl corrections.[30] Our Bader charge analysis predicts the amount of transferred charge to be about 0.3e per O atom. Note that the (transferred) excess charge fills the O_2 2p antibonding orbital, facilitating the O–O bond cleavage [B in Figure 2]. In contrast, there is a sizable barrier in the case of isolated DOSG (e.g., the calculated energy for O–O cleavage in $H_2Si < O_2$ is about 0.6 eV[12]). The resulting charge depletion in graphene can be demonstrated by the Fermi level downshift (Figure 3 b), as typically seen upon hole doping.[31]

In the following step [B → C], an O atom in DOSG reacts with a C atom in graphene to form an O–C linkage by crossing a barrier of about 0.33 eV, leading to rupture of a C–C π bond. The barrier was also estimated using LDA and GGA-PBE. The corresponding LDA and GGA values are 0.08 eV and 0.36 eV. Subsequently, the second O–C linkage is formed with no additional energy cost [D and E]. The DOSG + Gr → DOSG/Gr reaction is predicted to be exothermic by 0.79 (0.79, 1.60) eV according to the GGA-PW91 (GGA-PBE, LDA) calculation. It is noteworthy that LDA has a tendency to underestimate the barrier height and overestimate the binding strength. From our calculations, the moderate activation energy ($\approx$0.3 eV) and

 © 2011 Wiley-VCH Verlag GmbH & Co. KGaA, Weinheim

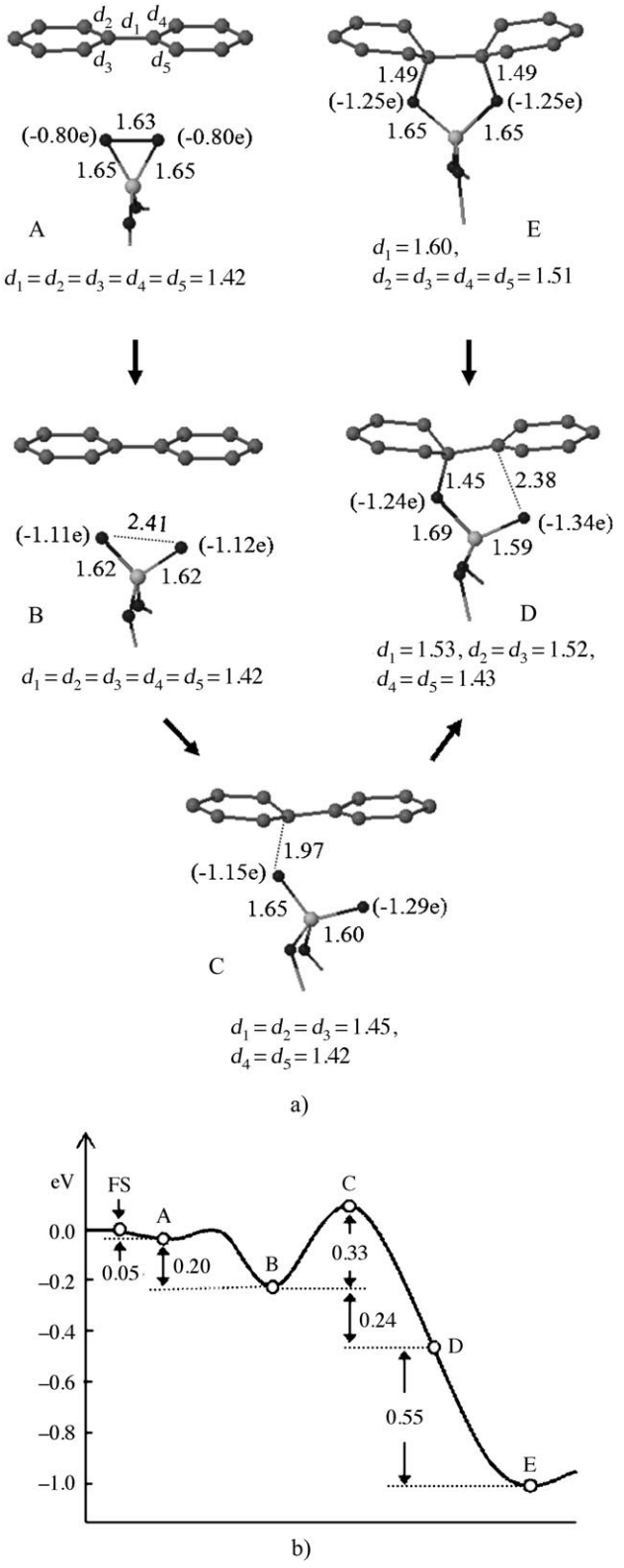

Figure 2. a) Predicted reaction pathway for DOSG binding to graphene and b) energy variation (in eV) along the reaction coordination from cluster DFT-GGA (PW91) calculations. The selected bond distances are given in Å, and the electronic charges of two terminal O atoms in DOSG are indicated in parenthesis. The light gray, dark gray, (small) white, and gray balls represent Si, O, H, and C, respectively.

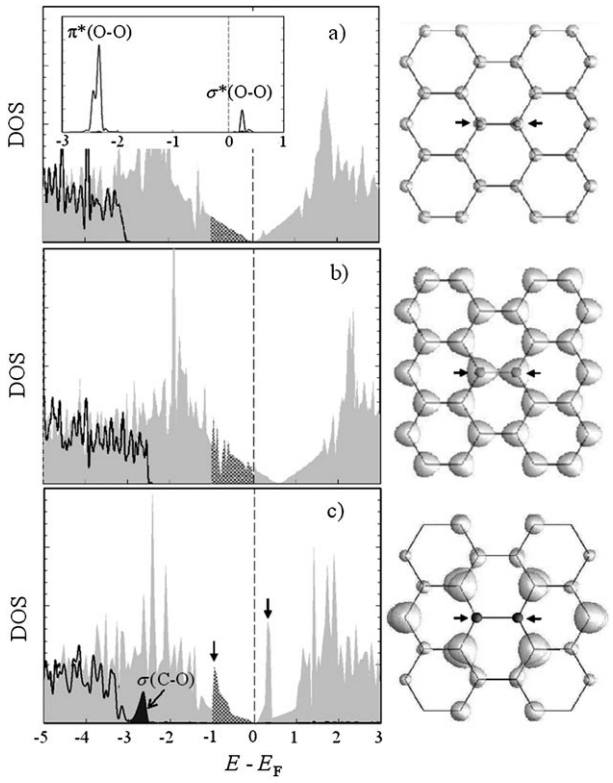

Figure 3. Electronic density of states (DOS, left panels) and isosurfaces (right panels) of decomposed charge densities corresponding to $E_F - 1\ eV < E < E_F$ (hatched area) for a) structure A, b) structure B, and c) structure E in Figure 2. The isosurface value is set to 0.02 electron Å^{-3}. Partial DOS projected on O_2 in DOSG is also presented in the inset of (a), demonstrating that the lowest unoccupied state, σ*(O–O), is located just above the Fermi level of the DOSG + graphene system. The vertical dotted line indicates the Fermi level position. The gray area represents p_z orbital and the solid lines indicate p_x and p_y orbitals, respectively. The sp^3 C atoms (bonded to DOSG) in graphene are represented by gray balls (also indicated by arrows), while the remaining sp^2 C atoms are presented by wireframe.

large exothermicity (≈0.8 eV) suggests the feasibility of the DOSG + Gr→DOSG/Gr reaction [A→E], even at room temperature.

Figure 3 also shows how the electronic structure of the DOSG-bonded graphene is modified as compared to free-standing graphene. For pristine graphene (Figure 3a), the honeycomb lattice consists of two identical interpenetrating triangular sublattices. Each of the C atoms is sp^2-hybridized to form three in-plane σ bonds while their p_z orbitals form π bonds. The π and π* bands exhibit a linear dispersion near the Dirac point, which is located at the Fermi level. In the DOSG/Gr case (Figure 3c), the sp^3 C atoms (in the C–O bonds) are decoupled from the π bands, perturbing the π conjugation network in their vicinity. This can be demonstrated by the occurrence of two distinct peaks at −0.9 eV and 0.3 eV in the DOS and corresponding decomposed charge density plots. A similar feature has been predicted upon the adsorption of two impurities on adjacent top sites[32] or a single impurity (such as S and O) on the bridge site.[33] The strong C–O bonding state appears about 2.6 eV below the Fermi level. Our calculations also sug-

 © 2011 Wiley-VCH Verlag GmbH & Co. KGaA, Weinheim

gest that the DOSG binding results in a possible gap opening (albeit very small) in graphene, and the DOSG/Gr structure is likely to have a zero net magnetic moment.

3. Conclusions

Herein, we have demonstrated the possibility of manipulating the nature of the binding interaction of graphene with *a*-SiO_2 by chemically modifying the *a*-SiO_2 surface, which might further contribute to tailoring the properties of the supported graphene. If dioxasilirane groups exist on *a*-SiO_2, our calculations show that graphene can be strongly bonded to the modified *a*-SiO_2 surface by forming Si–O–C linkages (while graphene typically weakly interacts with the defect-free surface through van der Waals forces). Our study also demonstrates that the dioxasilirane group can easily be formed by the adduction of molecular O_2 onto the terminal Si of a silylene center, which is an important surface defect in *a*-SiO_2. The DOSG–graphene bonding modifies the graphene electronic properties by perturbing the π conjugation network.

Acknowledgements

This work was supported by the R. A. Welch Foundation (F-1535). The authors also thank the Texas Advanced Computing Center for use of their computing resources.

Keywords: amorphous silica · covalent binding · density functional calculations · graphene · surface defect

[1] S. V. Morozov, K. S. Novoselov, A. K. Geim, *Phys.-Usp.* **2008**, *51*, 744 – 748.
[2] X. Liang, Z. Fu, S. Y. Chou, *Nano Lett.* **2007**, *7*, 3840 – 3844.
[3] D. Li, W. Windl, N. P. Padture, *Adv. Mater.* **2009**, *21*, 1243 – 1246.
[4] M. Ishigami, J. H. Chen, W. G. Cullen, M. S. Fuhrer, E. D. Williams, *Nano Lett.* **2007**, *7*, 1643 – 1648.
[5] J. C. Meyer, C. O. Girit, M. F. Crommie, A. Zettl, *Appl. Phys. Lett.* **2008**, *92*, 123110-1–123110-3.
[6] M. Z. Hossain, *Appl. Phys. Lett.* **2009**, *95*, 143125-1–143125-3.
[7] Y. J. Kang, J. Kang, K. J. Chang, *Phys. Rev. B* **2008**, *78*, 115404.
[8] T. O. Wehling, A. I. Lichtenstein, M. I. Katsnelson, *Appl. Phys. Lett.* **2008**, *93*, 202110 – 1–202110 – 3.
[9] L. Skuja, *J. Non-Cryst. Solids* **1998**, *239*, 16 – 48.
[10] Y. Xiong, S. Yao, R. Müller, M. Kaupp, M. Driess, *Nat. Chem.* **2010**, *2*, 577 – 580.
[11] K. Raghavachari, G. Pacchioni, *J. Chem. Phys.* **2001**, *114*, 4657 – 4662.
[12] N. Sawwan, A. Greer, *Chem. Rev.* **2007**, *107*, 3247 – 3285.
[13] D. G. Permenov, V. A. Radzig, *Kinet. Catal.* **2004**, *45*, 273 – 278.
[14] C. L. Kuo, G. S. Hwang, *Phys. Rev. Lett.* **2006**, *97*, 066101-1–066101-4; references cited therein.
[15] C. Morterra, M. J. D. Low, *Ann. N. Y. Acad. Sci.* **1973**, *220*, 133 – 244.
[16] J. P. Perdew, Y. Wang, *Phys. Rev. B* **1992**, *45*, 13244 – 13249.
[17] G. Kresse, J. Furthmüller, *VASP the Guide*, Vienna University of Technology, Vienna, **2001**.
[18] J. P. Perdew, K. Burke, M. Ernzerhof, *Phys. Rev. Lett.* **1996**, *77*, 3865 – 3868.
[19] D. M. Ceperley, B. J. Alder, *Phys. Rev. Lett.* **1980**, *45*, 566 – 569.
[20] P. E. Blöchl, *Phys. Rev. B* **1994**, *50*, 17953 – 17979.
[21] C. L. Kuo, S. Lee, G. S. Hwang, *Phys. Rev. Lett.* **2008**, *100*, 076104.
[22] H. J. Monkhorst, J. D. Pack, *Phys. Rev. B* **1976**, *13*, 5188 – 5192.
[23] G. Henkelman, A. Arnaldsson, H. Jónsson, *Comput. Mater. Sci.* **2006**, *36*, 354 – 360.
[24] G. Henkelman, B. P. Uberuaga, H. Jónsson, *J. Chem. Phys.* **2000**, *113*, 9901 – 9904.
[25] CPMD, Copyright IBM Corporation 1999 – 2001, Copyright MPI für Festkörperforschung, Stuttgart 1997 – 2004.
[26] H. Bornemann, W. Sander, *J. Am. Chem. Soc.* **2000**, *122*, 6727 – 6734.
[27] R. Becerra, S. J. Bowes, J. S. Ogden, J. P. Cannady, I. Adamovic, M. S. Gordon, M. J. Almond, R. Walsh, *Phys. Chem. Chem. Phys.* **2005**, *7*, 2900 – 2908.
[28] S. Nagase, T. Kudo, T. Akasaka, W. Ando, *Chem. Phys. Lett.* **1989**, *163*, 23 – 28.
[29] A. S. Zyubin, A. M. Mebel, S. H. Lin, Y. D. Glinka, *J. Chem. Phys.* **2002**, *116*, 9889 – 9896.
[30] P. E. Blöchl, O. Jepsen, O. K. Andersen, *Phys. Rev. B* **1994**, *49*, 16223 – 16233.
[31] I. Gierz, C. Riedl, U. Starke, C. R. Ast, K. Kern, *Nano Lett.* **2008**, *8*, 4603 – 4607.
[32] T. O. Wehling, M. I. Katsnelson, A. I. Lichtenstein, *Chem. Phys. Lett.* **2009**, *476*, 125 – 134.
[33] Y. G. Zhou, X. T. Zu, F. Gao, H. F. Lv, H. Y. Xiao, *Appl. Phys. Lett.* **2009**, *95*, 123119-1–123119-3.

Received: January 23, 2011
Revised: April 15, 2011
Published online on June 8, 2011

 © 2011 Wiley-VCH Verlag GmbH & Co. KGaA, Weinheim